Applied Scientific Research **51:** 55–59, 1993.
F.T.M. Nieuwstadt (ed.), Advances in Turbulence IV.

Spiral Vortices Between Concentric Cylinders

J. SÁNCHEZ, D. CRESPO, F. MARQUÈS
Dept. Física Aplicada. Universitat Politécnica de Catalunya.

Abstract. Spiral vortices appearing in Couette-Taylor flows are studied by means of numerical simulation. Transition curves from Couette to spiral vortices for different radius ratios and wavenumbers have been calculated in order to test our technique. Critical Reynolds numbers, angular velocities and slopes of the spirals at the onset of the instability agree with previous results [1]. Non-linear solutions obtained by a pseudospectral collocation method are studied, and they show a weak net axial flow. In order to counteract this effect, which is absent in the usual experimental set-up, an axial pressure gradient has been included. This procedure has proved to be sufficient to make the axial flow negligible. The onset of a quasiperiodic flow for larger Reynolds numbers, corresponding to a secondary bifurcation is also presented.

Keywords: Couette–Taylor system – spiral vortices – Hopf bifurcation – quasiperiodic flow

1. Introduction

Since the experimental work of Andereck et al. [2], counter-rotation has been known to produce a different primary instability; instead of Taylor vortex flow, Couette flow gives rise to spiral vortices, which are traveling waves in both the axial and azimuthal directions. The spiral vortex flow thus breaks both the continuous azimuthal and axial symmetries and is time periodic. In fact, it is a Hopf bifurcation of multiplicity two. Taylor-vortex flow is stable for a wide range of parameters. In contrast, spiral flow is stable only for a narrow interval, bifurcating towards interpenetrating laminar spirals which develop turbulent spots and spiral turbulence. In the present paper we report some results obtained by using a 2D numerical simulation in the region of parameters where spiral vortices appear.

2. Equations

The parameters that describe axially periodic Couette-Taylor systems are the radius ratio $\eta = R_i/R_o$ R_i and R_o being the inner and outer radius of the cylinders, and their Reynolds numbers Re_i and Re_o. In order to eliminate the pressure and the incompressibility condition from Navier-Stokes equations we write the velocity field in terms of two scalar potentials as $\mathbf{v} = \nabla \times (\overline{\psi}\hat{\mathbf{e}}_z) + \nabla \times \nabla \times (\overline{\phi}\hat{\mathbf{e}}_z)$. In [3] there is a detailed description of the set of evolution equations and boundary conditions for ψ and ϕ equivalent to Navier-Stokes equations. Here we suppose periodicity in the axial direction, so the domain under consideration in cylindrical coordinates is $(r, \theta_c, z) \in [R_i/d, R_o/d] \times [0, 2\pi] \times [0, 2\pi b]$, where b is the wavelength

in z direction and $d = R_i - R_o$. Double periodicity thus allows us to reduce the order of some of the equations and describe the velocity field as

$$\mathbf{v} = f\hat{\mathbf{e}}_\theta + g\hat{\mathbf{e}}_z + \nabla \times (h\hat{\mathbf{e}}_\theta + \psi\hat{\mathbf{e}}_z) + \nabla \times \nabla \times (\phi\hat{\mathbf{e}}_z) \tag{1}$$

where $f(r,z)$, $g(r,z)$, $h(r,\theta_c)$ are certain averages of the above-mentioned scalar potentials and ψ, ϕ are the remaining part of $\overline{\psi}$, $\overline{\phi}$.

To force spiral geometry we introduce the curvilinear coordinates $x = 2r - \delta$, $\theta_h = \theta_c$, $\rho = z/b - \theta_c$, $(x, \theta_h, \rho) \in [-1,1]\times[0,2\pi]\times[0,2\pi]$, where $\delta = (1+\eta)/(1-\eta)$. Functions depending only on x and ρ are invariant under combined rotation and axial shift movements, so they have helical symmetry. We therefore look for solutions independent of the θ_h coordinate in order to obtain spiral structures, so $\partial_{\theta_h} = 0$, $\partial_{\theta_c} = -\partial_\rho$, $\partial_z = \partial_\rho/b$. Thus the dependency of the potentials is $f = f(r)$, $g = g(r)$, $h = 0$, $\psi = \psi(r,\rho)$, $\phi = \phi(r,\rho)$, and the equations take the form

$$(\partial_t - DD_+)f = -P_\rho\hat{\mathbf{e}}_\theta \cdot \boldsymbol{\omega} \times \mathbf{v} \tag{2}$$

$$(\partial_t - D_+D)g = -P_\rho\hat{\mathbf{e}}_z \cdot \boldsymbol{\omega} \times \mathbf{v} \tag{3}$$

$$(\partial_t - \Delta)\Delta_h\psi = (1 - P_\rho)\hat{\mathbf{e}}_z \cdot \nabla \times \boldsymbol{\omega} \times \mathbf{v} \tag{4}$$

$$(\partial_t - \Delta)\Delta\Delta_h\phi = -(1 - P_\rho)\hat{\mathbf{e}}_z\nabla \times \nabla \times \boldsymbol{\omega} \times \mathbf{v} \tag{5}$$

with $\boldsymbol{\omega} = \nabla \times \mathbf{v}$, $D = \partial_r$, $D_+ = D + 1/r$, $\Delta_h = D_+D + 1/r^2\partial^2_{\rho\rho}$, $\Delta = \Delta_h + 1/b^2\partial^2_{\rho\rho}$ $P_\theta = P_\rho$ being the θ and ρ average operators. Boundary conditions are

$$f(R_i) = Re_i,\ f(R_o) = Re_o \quad \text{and} \quad g = 0, \tag{6}$$

$$D\psi = \phi = \Delta_h\phi = -b\psi + rD\phi = b\Delta\Delta_h\phi + rD\Delta_h\psi = 0 \text{ on } r = R_i, R_o \tag{7}$$

f, g are the mean velocities in the azimuthal and axial directions, averaged with respect to θ and z coordinates.

3. Linear stability analysis

In this section we study the linear stability of the Couette flow defined by $\mathbf{v}_c = f_c\hat{\mathbf{e}}_\theta$, $f_c = Ar + B/r$ and $g_c = \psi_c = \phi_c = 0$ with

$$A = \frac{Re_o - \eta Re_i}{1+\eta},\ B = \frac{\eta(Re_i - \eta Re_o)}{(1+\eta)(1-\eta)^2}. \tag{8}$$

By linearizing equations (2) to (5) about f_c and trying out solutions of the form $\psi(r,\rho,t) = \psi(r)e^{\lambda t + in\rho}$, $\phi(r,\rho,t) = \phi(r)e^{\lambda t + in\rho}$, we obtain the eigenvalue problem

$$\lambda\Delta_h\psi = \Delta\Delta_h\psi + in(\frac{2A}{b}\Delta_h\phi + \frac{f_c}{r}\Delta_h\psi) \tag{9}$$

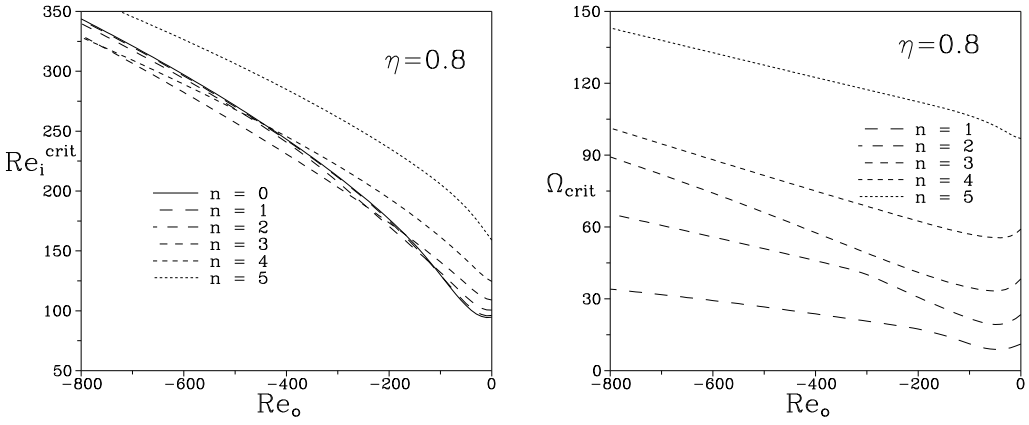

Fig. 1. Linear analysis curves.

$$\lambda\Delta\Delta_h\phi = \Delta\Delta\Delta_h\phi - in(\frac{2f_c}{br}\Delta_h\psi + \frac{4Bn^2}{br^4}\psi \\ -\frac{4B}{br^3}\psi_r - \frac{f_c}{r}\Delta\Delta_h\phi + \frac{4B}{r^3}D_-\Delta\phi) \tag{10}$$

with boundary conditions (7), and $n \neq 0$ because $P_\rho\psi = P_\rho\phi = 0$. In this eigenvalue problem equations for f and g are diffusion ones and do not contribute to the instability, so the perturbation of $\mathbf{v}_c$ is $\mathbf{v} = \nabla \times (\psi\hat{\mathbf{e}}_z) + \nabla \times \nabla \times (\phi\hat{\mathbf{e}}_z)$.

Notice that now eigenvalues and eigenfunctions depend on a fourth parameter b in adition to Re_i, Re_o, η. For some values of the radius ratio η we have determined the curves of critical inner Reynolds number Re_i^{crit}, the slope b^{crit} and the rotation frequency at the onset of spirals, all as functions of the outer Reynolds number Re_o. Curves of Re_i^{crit} and Ω^{crit} are shown in Fig. 1 for $\eta = 0.8$. Our results agree with those from [1].

The eigenvalue problem has been discretized using a Tchebychev collocation method.

4. Non-linear solutions

Equations derived from (2) to (7) for the perturbation of the Couette flow were solved by using a semi-implicit first order Euler-Adams-Bashforth scheme for time integration and a pseudospectral collocation method for the spatial discretization. The potentials are expanded in trigonometric functions for the ρ coordinate and Tchebychev polinomials for the radial dependence. (See [4] and [5] for details).

The transition from Couette flow to spiral vortices is a Hopf bifurcation giving rise to periodic attractive orbits. Fig. 2.b shows the velocity field corresponding to $\eta = 0.8$, $Reo = -124$, $Rei = 180$ and $b = 0.375$ (see Fig. 1). The spirals in a couple are of different size, in contrast with the Taylor-vortex flow. The difference is also

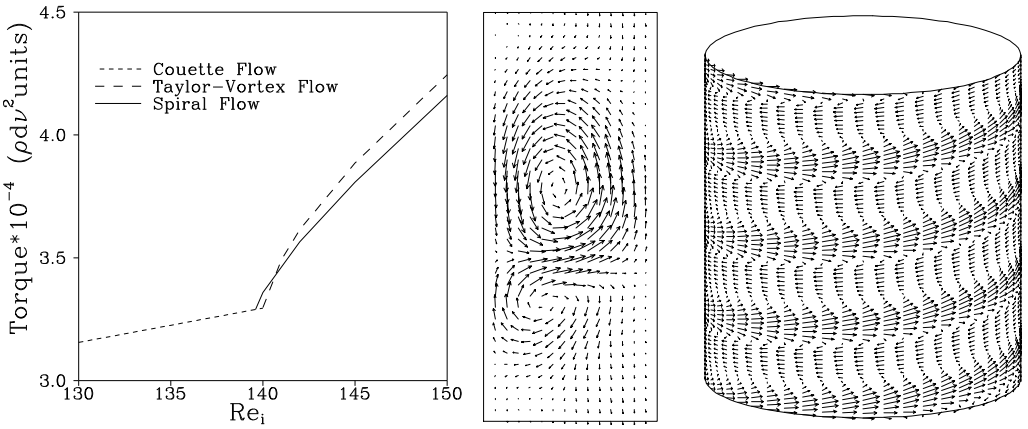

Fig. 2. a) Torque exerted by the fluid on the outer cylinder. Projections of the velocity field onto constant θ and r sections, b) and c).

reflected in Fig. 2.c, showing the velocity field on the cylinder $r = r_i + 0.6d$. This is related to the breaking of the symmetry about a z-constant plane. A strong outgoing jet appears between the spirals. This is due to the centrifugal instability mechanism, as in the Taylor-vortex flow. Lid effects must be mentioned at this point. The solutions calculated have a small net mean vertical flow due to non-zero volume-average of g. A vertical pressure gradient has been added to the equations in order to cancel it. The pressure head simulates the real laboratory flows, with cylinders of finite length where a mean flow cannot exist, and the lids may supply an axial pressure gradient. Solutions including the pressure head are almost identical to the previously computed ones except for the mean flow. We have also computed the torque exerted on the cylinders. Fig. 2.a shows the torque exerted in the Couette flow, Spirals and Taylor-vortex cases. The results show that the spiral flow transpors angular momentum more efficiently near the bifurcation, but Taylor-vortex are more efficient for higher Reynolds numbers.

Fig. 3 shows two-dimensional projections of the phase portrait and power spectra of solutions obtained by fixing Re_o and increasing Re_i. The onset of a new frequency giving rise to a quasiperiodic flow corresponds to a secondary bifurcation. This new regime appears in a region where two spiral flows with a different slope b appear in the primary bifurcation.

5. Discussion

Some new important features have been obtained, such as the presence of a weak axial flux and a secondary bifurcation to a quasiperiodic flow near the primary instability. The weak axial flow is due to the symmetry breaking primary bifurcation. The presence of a quasiperiodic flow near the instability is caused by

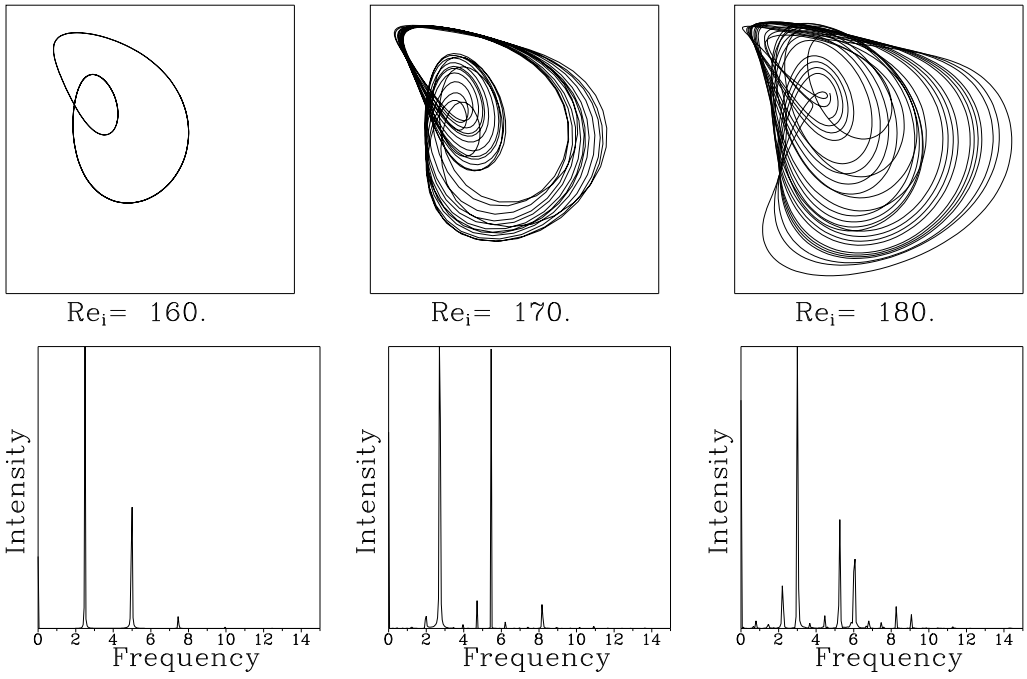

Fig. 3. Transition from periodic to quasiperiodic orbits when Re_i is increased. Frequency is measured in Hz.

the competition between different spiral modes. The reliability of the computed flows is being tested experimentally by using image processing techniques. The results will be published elsewhere.

Our 2D model captures some relevant aspects of the bifurcations in the counter-rotating case. Additional improvements would include a fully 3D code in order to break the helical symmetry of the present model.

References

1. W.F. Langford, R. Tagg, E. J. Kostelich, H.L. Swinney, and M. Golubitsky 1988 'Primary instabilities and bicriticality in flow between counter-rotating cylinders.' *Phys. Fluids* **vol. 31**, 776
2. C.D. Andereck, S.S. Liu, H.L. Swinney. 1986 'Flow regimes in a circular Couette system with independently rotating cylinders.' *J. Fluid Mechanics* **vol. 164**, 155
3. F.Marquès. 1990 'On boundary condition for velocity flows: Application to Couette flow.' *Phys. Fluids A* **2**, 729
4. C. Canuto, M. Yousuff Hussaini, A. Quarteroni, and T.A. Zang. 1988 'Spectral Methods in Fluid Dynamics' Springer-Verlag.
5. F.Marquès, I. Mercader, M. Net and J Massaguer. 1992 'Thermal convection in vertical cylinders. A method based on potentials of velocity.' *Computer Meths Appl Mech Engng. (submitted).*